Available online at www.CivileJournal.org

Civil Engineering Journal

(E-ISSN: 2476-3055; ISSN: 2676-6957)

Vol. 8, No. 12, December, 2022

Simulation of Hybrid Mesh Turbomachinery using CFD and Additive Technologies

Yuri A. Sazonov [1], Mikhail A. Mokhov [2*], Inna V. Gryaznova [3], Victoria V. Voronova [3], Khoren A. Tumanyan [2], Mikhail A. Frankov [4], Nikolay N. Balaka [5]

[1] *Department of Machinery and Equipment of the Oil and Gas Industry, National University of Oil and Gas, Gubkin University, Moscow, Russia.*

[2] *Department of Development and Operation of Oil Fields, National University of Oil and Gas, Gubkin University, Moscow, Russia.*

[3] *Development of Gas and Gas Condensate Fields, National University of Oil and Gas, Gubkin University, Moscow, Russia.*

[4] *Institute of Petrophysics, National University of Oil and Gas, Gubkin University, Moscow, Russia.*

[5] *Head of Department for Technological Support of Well Construction, CJSC: Russian Company for Shelf Development, Moscow, Russia.*

Received 14 September 2022; Revised 25 November 2022; Accepted 28 November 2022; Published 01 December 2022

Abstract

This paper develops schematics and evaluates the performance of hybrid mesh turbomachinery at the patenting stage of individual technical solutions. This type of turbomachine uses reduced-sized blades and also forms flow channels with a mesh structure between the blades. The research methods are based on simulations using computational fluid dynamics (CFD) and additive technologies. An intermediate conclusion is that a new scientific direction for investigating and creating hybrid mesh turbomachinery equipped with mesh jet control systems was formed to develop Euler's ideas. This paper describes new possibilities for the simultaneous implementation of two workflows in a single impeller: 1) Turbine workflow, and 2) Compressor workflow. Calculation methods showed possible improvements in the performance of the new turbomachines. This paper considers options for mesh turbomachine operation in the two-stage gas generator mode with partial involvement of atmospheric air in the workflow. Preliminary calculations based on examples show that it is possible to expect a two- to four-times increase in thrust when using hybrid mesh turbomachines. Ongoing studies mainly focus on developing multi-mode turbomachinery that works in complicated conditions, such as offshore oil and gas fields, but some research results are applicable in other industries, for example, in developing hybrid propulsion systems or propulsors.

Keywords: Mesh Turbomachine; Turbine; Compressor; Research; Simulation; Patenting; Computational Fluid Dynamics.

1. Introduction

Within the framework of mechanical engineering science, the most relevant problem is finding ways to increase the specific performance of machines with a rational use of energy. To solve this problem and develop Euler's ideas, specialists at Gubkin University carried out a series of research studies on developing hybrid mesh turbomachines [1–6]. In these machines, flow channels have a mesh structure. In common understanding, a mesh represents a larger geometric area by having smaller discrete cells. In a mesh turbomachine, a set of smaller blades replaces blades of a larger size through the formation of flow channels in the form of a mesh structure.

Studies have revealed new possibilities for controlling the flows of gases and liquids [5]. The control range for the deflection angle of the velocity vector (thrust vector) at the gas (liquid) outlet from the nozzle has been extended [1, 5]. It has been shown that this deflection angle of the velocity vector can take on any value within a geometric sphere. These

* Corresponding author: mikhal.mokhov@mail.ru

http://dx.doi.org/10.28991/CEJ-2022-08-12-011

scientific developments can be used in the creation of new mesh turbomachines capable of working in complicated conditions, including gas-liquid media. Analysis of scientific publications shows that this area of turbomachinery remains poorly studied. The authors of this paper propose to pay attention to the emerging opportunities for implementing two working processes in one impeller (turbine workflow and pump workflow). Here, it is reasonable to evaluate and consider the main trends of modern development in the field of turbomachinery and control systems (from different industries).

Studies have revealed new possibilities for controlling the flows of gases and liquids [5]. The control range for the deflection angle of the velocity vector (thrust vector) at the gas (liquid) outlet from the nozzle has been extended [1, 5]. It has been shown that this deflection angle of the velocity vector can take any value within a geometric sphere. These scientific developments can be used in the creation of new mesh turbomachines capable of working in complicated conditions, including gas-liquid media. An analysis of scientific publications shows that this area of turbomachinery still remains poorly studied. The authors of this paper propose to pay attention to the emerging opportunities for implementing two working processes in one impeller (turbine workflow and pump workflow). Here, it is reasonable to evaluate and consider the main trends of modern development in the field of turbomachinery and control systems (from different industries).

It is well-known that production systems for oil and gas production, transportation, and refining actively use advanced scientific developments from other industries, including aviation technologies and modified aircraft engines. In this regard, conducting a system analysis of structures and generalizing experience in machine design is not limited to any one industry, and the issues are considered from the general positions of the mechanical engineering science.

Currently, the mesh structures are studied mainly to reduce the product weight while preserving their strength characteristics [7, 8]. Note that modern additive technologies maximize the rigidity of the rotor structure while minimizing the rotor mass [9-11], which is essential for controlling the vibration activity of rotating parts and units. Using additive technology, it is now also possible to create complex compositions of metallic and ceramic materials that are difficult or impossible to obtain in other ways [12]. The peculiarities of gas-dynamic processes in creating lattice wings [13-15] and aircraft [16-18] have been studied. Parts of modern turbines experience high thermal loads [19–21], which require finding new solutions for designing cooled blades. The leading edge is a critical area of a gas turbine blade and is often insufficiently cooled [22].

Hybrid systems containing two engines based on different physical principles have been actively discussed [23-25]. Engines are equipped with special nozzles for the thrust vector control [26, 27]. The features of the flows at the nozzle outlet have been studied [28-30]. Research into hydrogen fuel [31] and detonation engines has intensified [32]. The presented scientific developments and technical achievements are now considered from the position of their applicability in the development of promising mesh turbomachines.

The authors of this paper developed and published the following hypothesis [1–6]: it is advisable to develop energy-saving technologies and techniques at the junction of two scientific and technical directions: the first direction relates to mesh hybrid turbomachines, the second - to jet control systems to control the velocity vector (thrust vector). The mesh structure of the turbo-machine flow path provides strength and rigidity to the rotor structure with a low mass. The jet control system has high reliability (due to the small number of moving parts) with a low mass of the entire system.

The main project objectives within this scientific paper are to identify promising areas of technology and engineering development using hybrid mesh turbomachines and new opportunities to improve the methodology of designing turbomachines within the training of modern designers. Ongoing studies mainly focus on developing multi-mode turbomachinery working in complicated conditions, such as offshore oil and gas fields. However, some research results are applicable to solving practical tasks in other industries, including increasing the efficiency of energy conversion processes, electric power generation, aviation, and marine transportation systems.

2. Methods

The research object is a set of gas-dynamic and hydrodynamic processes at different flow modes through rotating and stationary channels with a mesh structure. This paper develops schematics and evaluates the performance of hybrid mesh turbomachinery at the patenting stage of individual technical solutions. The methods and methodology of this work are experimental and theoretical methods for studying gas-dynamic and hydrodynamic processes, including computer simulation use, prototyping methodologies, and additive technologies. This scientific research used a well-known interdisciplinary approach and methodology [33], always considering a set of the following processes and conditions:

- Blade and vortex, pump (or compressor) and turbine workflows;
- Coalescence and dispersion processes, cavitation in liquid and gas-liquid mixtures, separation in multiphase media;
- Workflows in the presence of solid particles in a fluid flow, at a point or distributed power input, at series and parallel connection of machines, in one-stage or multistage machinery, flow processes considering hydraulic friction and impact losses with partial pressure recovery at constant and variable resistance coefficients;

- The development or attenuation of individual hydrodynamic (gas-dynamic) processes in different points of the engine working chamber when changing the parameters of the working fluid;
- The features of changes in the physical properties of the liquid or gas-liquid mixture at different points in the machine flow path;
- Conditions of presence (or absence) of axial symmetry for solid walls in flow channels (and for the fluid flow), conditions and methods used for machine regulation, conditions for steady (or impulse) flow regime in individual zones and flow channels.

Figure 1 shows a flowchart of the research methodology.

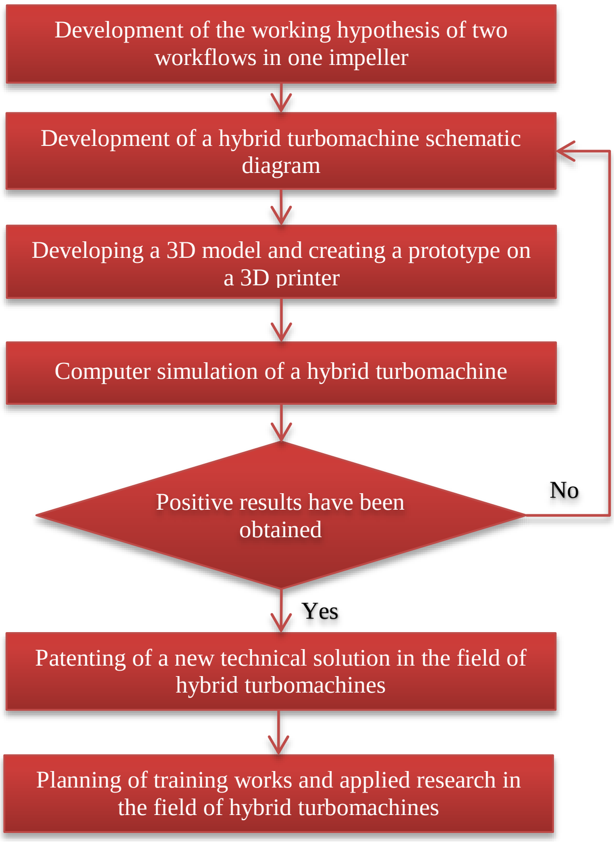

Figure 1. Flowchart of the research methodology

3. Results and Discussions

3.1. Development of Schematics for Hybrid Mesh Turbomachinery

The ongoing research considers new approaches for developing special hybrid turbomachines with the simultaneous implementation of turbine and pump (or compressor) workflows in the flow channels of one impeller. It also searches for ways to increase specific indicators of machines with reasonable energy use. Figure 2 shows a new scheme to describe the developed and patented turbomachine [6] under the RF utility model patent No. 213280.

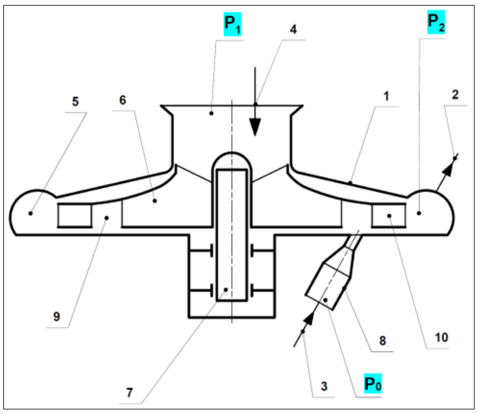

Figure 2. Scheme of the developed and patented turbomachine [6] under the RF utility model patent No. 213280: 1 – casing; 2 – outlet channel (pressure P_2); 3 – working fluid inlet channel (pressure P_0); 4 – pumped fluid inlet channel (pressure P_1); 5 – mixing chamber; 6 – impeller; 7 – shaft; 8 – nozzle diaphragm; 9 – annular channel; 10 – turbine blades.

This turbomachine belongs to the field of pumping and compressor technology and is designed to pump liquids, gases, and their mixtures and is also applicable for developing thermal machines. Figure 3 shows a scheme of the impeller [6] under the RF utility model patent No. 213280.

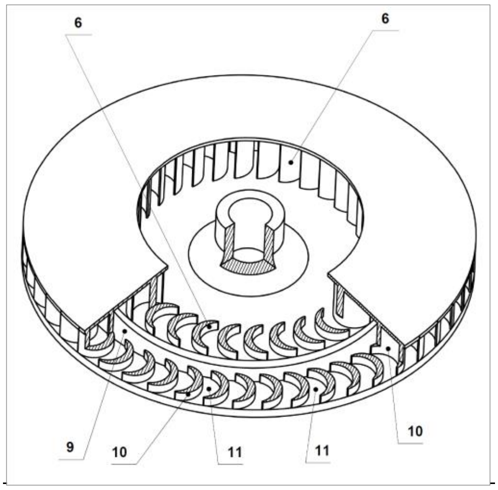

Figure 3. Scheme of the impeller

The impeller 6 is equipped with a system of turbine blades 10. Flow channels 11 hydraulically connect the annular channel 9 with outlet channel 2. Turbine blades 10 can form a mesh structure. The mesh structure provides higher structural rigidity and strength with its low weight. Figure 4 shows a schematic unfolding of the impeller blade system [6] under the RF utility model patent No. 213280.

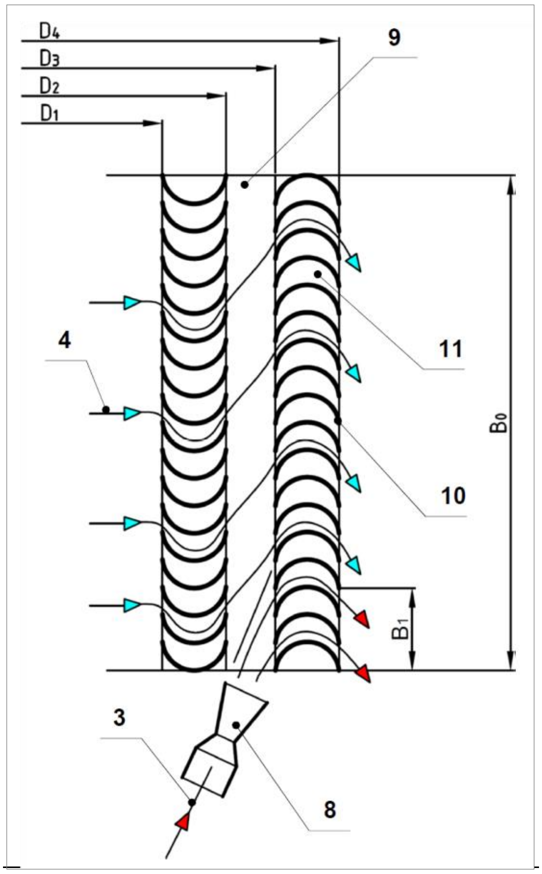

Figure 4. Schematic unfolding of the impeller blade system

The outlet edges of blades 10 are on a circle of diameter D_4. In the scheme, the segment B_0 corresponds to the circumference with the diameter D_4, or $B_0 = \pi D_4$. The working fluid flow coming out of the nozzle 8 interacts with the blades 10 when these blades, during their motion, overcome the path segment B_1. Figure 5 shows the impeller with a nozzle diaphragm [6, 34] under the RF utility model patent No. 213280, No. 214113.

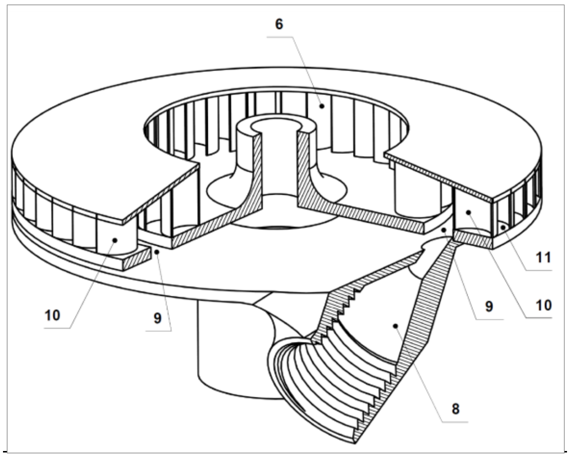

(a)

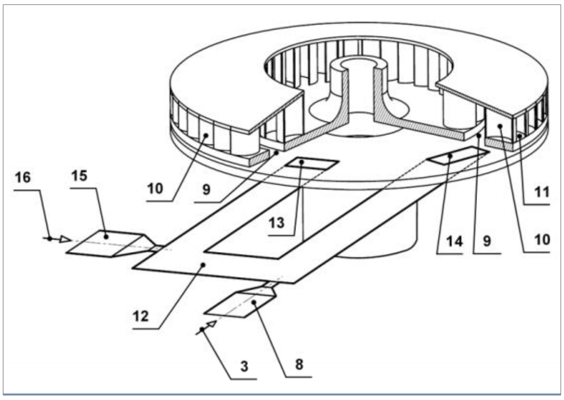

(b)

Figure 5. Impeller with nozzle diaphragm in the assembly (3D model – isometric): a - Patent No. 213280 [6]; b – Patent No. 214113 [34]

The fluid flow regime through the nozzle diaphragm 8 can be stationary or pulsed, depending on the current technical problem. The nozzle diaphragm 8 can have several outlets directed toward the turbine blades 10. To supply additional power, the shaft 7 can be connected to an additional engine (internal combustion engine or electric motor, not shown in the drawings), depending on the technical problem to be solved. To remove excessive power, the shaft 7 can be connected to an additional machine (electric generator, additional compressor, or pump, not shown in the drawings), depending on the technical problem to be solved.

A variant of the turbomachine (Figure 5b) is also possible where the nozzle diaphragm 8 is connected to the flow-through mixing heat exchange tube 12 with the possibility of pre-mixing the hot working medium with the cold pumped medium, where the inlet 13 and outlet 14 of the flow-through mixing heat exchange tube 12 communicate with the annular channel 9 and the mixing chamber 5. The flow mode of the working medium through the nozzle diaphragm 8 and through the flow-through mixing heat exchange tube 12 can be stationary or pulsed, depending on the technical problem to be solved. The nozzle diaphragm 8 can have several outlets directed to the turbine blades 10, depending on the technical problem to be solved. Variants using two (or more) flow-through mixing heat exchange tubes 12 are possible. For example, the flow-through mixing heat exchange tube 12 can also have an additional nozzle diaphragm 15 with an inlet channel 16 to activate the heat exchange processes [34].

The turbomachine works as follows (Figures 2 to 5). Through the inlet channel 3, the working fluid (liquid, gas, or gas-liquid mixture with high temperature) under pressure enters the nozzle diaphragm 8. A high-temperature jet of the working fluid, coming out from the nozzle diaphragm 8, forces the turbine blades 10, making the impeller 6 to rotate. Rotating impeller 6 forces on the pumped fluid and generates the pumped fluid (liquid, gas, or gas-liquid mixture) flow while the temperature of the pumped fluid can be significantly lower than that of the working fluid. Pumped fluid enters through the inlet channel 4, passes through the impeller and its flow channels 11, and discharges through the outlet channel 2. The working fluid passes through the flow channels 11 and mixes with the pumped fluid and discharges through the output channel 2.

Thus, rotating impeller 6 equipped with a system of turbine blades 10 performs energy transfer from the working fluid to the pumped fluid. As the impeller 6 and turbine blades 10 rotate, either a flow of working fluid or pumped fluid periodically passes through flow channels 11. The high-temperature fluid flow heats the turbine blades 10, and the cooler pumped fluid flow removes heat and cools the turbine blades 10.

Due to favorable cooling conditions of turbine blades 10, it becomes possible to increase the working fluid (gas) temperature, which promotes the increase in efficiency of the workflow in the turbomachine, for example, for a thermal machine, when the pumped fluid is cold air, and the working fluid is the hot gas from a gas generator. Thus, the technical results improve the cooling conditions of turbine blades with the possibility of increasing the temperature of working gas and the efficiency of energy conversion in the flow path of the turbomachine.

3.2. Application of Additive Technologies to Developing Micromodels (Prototypes)

Figures 6 and 7 show photos of the turbomachine prototype under the RF utility model patent No. 213280 [6] developed using additive technologies, according to the schematics in Figures 2 to 5.

Figure 6. Photo of the turbomachine prototype (variant)

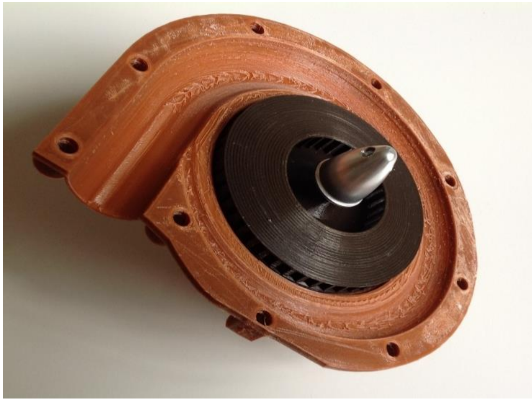

Figure 7. Photo of the turbomachine prototype (after removing the upper part of the casing)

In such a turbomachine, the nozzle diaphragm can have a velocity vector (thrust vector) control system. This paper does not consider such a system, but other authors' publications described it [1–5].

3.3. Discussion of Approaches to the Calculation of Hybrid Machines Based on the Existing Theoretical Basis

It is well-known that after the emergence of a patentable idea, an immediate need arises to verify the performance of a new technical solution. For this purpose, the first schematics and the first computational scheme for preliminary calculations are usually developed. According to the computational scheme, a mathematical model is developed, refined and complicated during research and design work. Let us consider the simplified scheme of the turbomachine (jet system), which implements the interaction of working and pumped fluids (Figure 8).

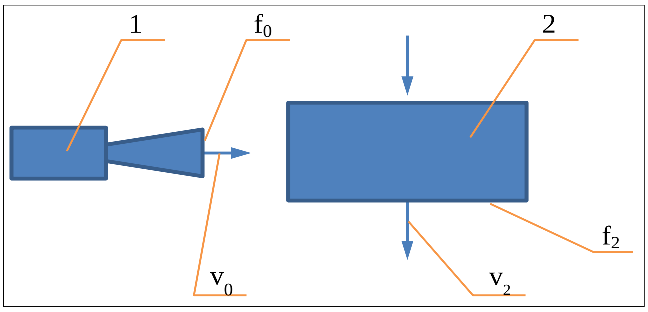

Figure 8. Scheme of the jet system for the energy converter: 1 – working fluid source, 2 –working chamber

Let us consider the mathematical model variant for the presented idealized jet system. The working fluid source (or gas generator) 1 makes it possible to form a jet of the working fluid at flow velocity v_0 in the outlet cross-section with area f_0 with the density of the working fluid ρ_0; the volume flow rate of the working fluid $Q_0 = f_0 v_0$, and the mass flow rate of the working fluid $\dot{Q}_0 = Q_0 \rho_0$. The reactive force (or thrust – in aviation terminology) at the flow of the working fluid is known to be determined by the relationship $F_0 = Q_0 \rho_0 v_0$.

Working chamber 2 serves for energy conversion and forces the pumped fluid flow. It can have ejector/turbofan (turbocharger) or other machines. At the outlet of the working chamber 2, a jet at a flow velocity v_2 in the outlet cross-section area f_2 with the density of the pumped fluid ρ_2 (or the pumped and working fluid mixture) is formed. Here, the volume flow rate at the outlet of the chamber 2 is$Q_2 = f_2 v_2$ mass flow rate – $\dot{Q}_2 = Q_2 \rho_2$, respectively. The reactive force or thrust at the outlet of the chamber 2 is determined using the formula $F_2 = Q_2 \rho_2 v_2$. As is known, the kinetic energy of the fluid flow can be estimated through the power parameter as follows.

$$N_0 = Q_0 \rho_0 \frac{v_0^2}{2} \tag{1}$$

The kinetic energy of the flow at the outlet of the chamber 2 can be estimated through the power parameter:

$$N_2 = Q_2 \rho_2 \frac{v_2^2}{2} \tag{2}$$

The ratio of the volume flow rates is:

$$q = \frac{Q_2}{Q_0} \tag{3}$$

The coefficient of thrust amplification (change) is:

$$K_F = \frac{F_2}{F_0} \tag{4}$$

Publications [1–5] previously presented the results of laboratory tests of micromodels of mesh turbomachines and confirmed the performance of new technical solutions by recording of K_F coefficient values ranging from 1.9 to 2.1 when testing micromodels in the air in the turbofan mode. Figure 9 schematically presents variant 1 of the turbomachines shown in more detail in Figures 1 to 4. The flow with a volume flow rate Q_{01} from the working fluid source (or from an additional fluid source with Q_{02}) is directed into the rotor channels. The pumped fluid with a volume flow rate Q_1 goes to the rotor center. The working and pumped fluid mixture with a volume flow rate Q_2 discharges through the outlet channel.

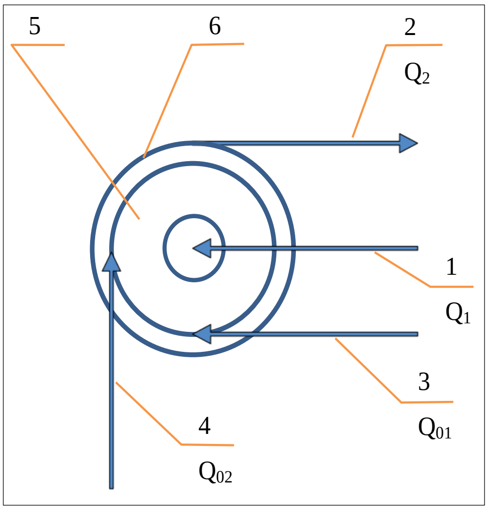

Figure 9. Scheme of turbomachine (variant 1): 1 – inlet channel for pumped fluid; 2 – outlet channel for the mixture of working and pumped fluids; 3, 4 – inlet channels for working fluid; 5 – rotor; 6 – casing

According to Figure 9, the flow with a volume flow rate Q_{01} from the working fluid source 3 (or from an additional fluid source withQ_{02}) is directed into the rotor channels. The pumped fluid with a volume flow rate Q_1 goes from inlet channel 1 to the center of the rotor 5. The working and pumped fluid mixture with a volume flow rate Q_2 discharges from casing 6 through the outlet channel 2. At the turbomachine outlet, a heat exchange chamber or an afterburner chamber with the supply of thermal energy L_2 can be installed (Figure 10, variant 2).

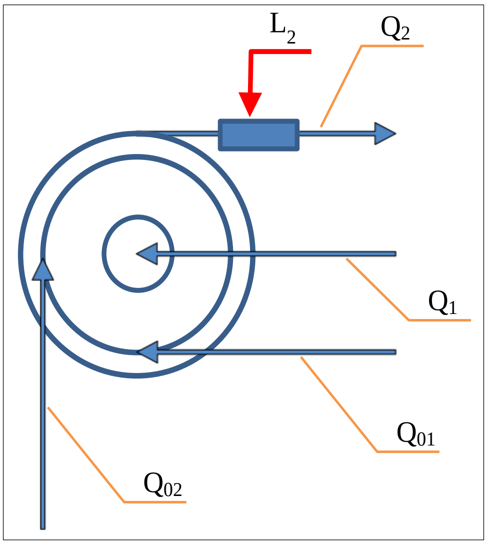

Figure 10. Scheme of the turbomachine (variant 2)

The following symbols are used for gas fluid operating conditions. Absolute gas temperatures at the turbine inlet is T_0 and outlet $-T_{20}$, compressor inlet $-T_1$ and outlet $-T_{21}$, and at the mixing chamber outlet $-T_3$. Adiabatic exponents $-k_0$, k_1, k_3; gas constants $-R_0$, R_1, R_3; and average isobaric heat capacities $-c_{p0}$, c_{p1}, c_{p3} for the flow through the turbine, compressor and mixing chamber, respectively. Efficiency factors for the turbine and compressor $-\eta_0$, and η_1, respectively. The gas mass flow rate through the turbine $-\dot{Q}_0$ and compressor $-\dot{Q}_1$. The power of additional energy source, e.g., additional engine$-N_3$ (connected to the rotor shaft); power of additional heat source $-L_2$ (as applied to the schemes in Figures 2 to 5, 9, 10). Gas pressure at the turbine inlet is P_0 and outlet $-P_2$, at the compressor inlet $-P_1$ and outlet $-P_2$.

Here, the turbomachine variants are predominantly considered for the following conditions.

$$T_0 > T_{20} > T_1 \tag{5}$$

$$T_0 > T_{21} > T_1 \tag{6}$$

The gas, leaving the compressor with a temperature of T_{21} periodically directly cools the turbine blades. If we denote the total turbine operation time by x_0 and the overall cooling time of these blades by x_2, then it is possible to introduce a dimensionless parameter X characterizing the cooling conditions of the turbine blades:

$$X = \frac{x_2}{x_0} \tag{7}$$

When discussing the presented topic, it is possible to use the well-known mathematical dependencies, usually used for various thermal machines and turbojet engines [35, 36]. The degree of pressure reduction in the turbine is

$$\pi_0 = \frac{P_0}{P_2} \tag{8}$$

The degree of pressure increase in the compressor is:

$$\pi_1 = \frac{P_2}{P_1} \tag{9}$$

The specific work of the turbine is:

$$l_0 = \frac{k_0}{k_0 - 1} R_0 T_0 \left(1 - \pi_0^{\frac{1-k_0}{k_0}}\right) \eta_0 \tag{10}$$

The specific work of the compressor is:

$$l_1 = \frac{k_1}{k_1 - 1} R_1 T_1 \left(\pi_1^{\frac{k_1-1}{k_1}} - 1\right) \eta_1^{-1} \tag{11}$$

The ratio of the mass flow rates is:

$$\dot{q} = \frac{\dot{Q}_1}{\dot{Q}_0} \tag{12}$$

The specific work of the additional engine is:

$$l_3 = \frac{N_3}{\dot{Q}_0} \tag{13}$$

The specific work balance is:

$$l_3 + l_0 = \dot{q} l_1 \tag{14}$$

$$\frac{N_3}{\dot{Q}_0} + \frac{k_0}{k_0-1} R_0 T_0 \left(1 - \pi_0^{\frac{1-k_0}{k_0}}\right) \eta_0 = \dot{q} \frac{k_1}{k_1-1} R_1 T_1 \left(\pi_1^{\frac{k_1-1}{k_1}} - 1\right) \eta_1^{-1} \tag{15}$$

Note that a separate rotor blade in the new mesh turbomachine periodically participates in the turbine and compressor workflows. This peculiarity of the workflow should be considered in developing new theories and software for such mesh machines.

The thermal balance of the mixing chamber is:

$$\dot{Q}_0 c_{p0} T_{20} + \dot{Q}_1 c_{p1} T_{21} + L_2 = (\dot{Q}_0 + \dot{Q}_1) c_{p3} T_3 \tag{16}$$

Gas temperature after the turbine is:

$$T_{20} = T_0 \left(1 - \left(1 - \pi_0^{\frac{1-k_0}{k_0}}\right) \eta_0\right) \tag{17}$$

Gas temperature after the compressor is:

$$T_{21} = T_1 \left(1 + \left(\pi_1^{\frac{k_1-1}{k_1}} - 1\right) \eta_1^{-1}\right) \tag{18}$$

It is well-known that restrictions on the gas velocity and temperature at the turbomachine outlet can be (for example, for some aircraft with vertical takeoff and landing). In this regard, when calculating and considering mesh turbomachines, it is necessary to choose individual or complex optimization criteria, considering the conditions for the specific application problem.

The patenting stage of the technical solution included calculations confirming the operability of the proposed turbomachine (Figures 2 to 5). Tables 1 to 3 partially present information on them. In calculations 1 and 2, the working gas is methane (such as gas from a gas well with high reservoir pressure), and the pumped gas is also methane (such as gas from a gas well with low reservoir pressure).The pumped gas (methane) temperature at the compressor inlet is $T_1 = 300$ К, the gas constant $R_0 = R_1 = 523$ J/(kg $*$ K),adiabatic exponents$k_0 = k_1 = 1.31$,isobaric heat capacities $c_{p0} = c_{p1} = 2483$ J/(kg $*$ K),and the pressure variation range is 0.2 MPa $\leq P_1 \leq 0.5$ MPa. Here, the pressure increase in the compressor is $1.2 \leq \pi_1 \leq 3$, where $\pi_1 = P_2/P_1$.

Table 1. Initial data and results of calculation 1

№	T_0	P_0	P_1	P_2	P_2/P_1	$\dot{Q}_0$	$\dot{Q}_1$	$\dot{Q}_1/\dot{Q}_0$
	К	MPa	MPa	MPa	/	kg/s	kg/s	/
1	300	10	0.20	0.60	3.00	1	0.57	0.57
2	300	10	0.25	0.60	2.40	1	0.74	0.74
3	300	10	0.30	0.60	2.00	1	0.95	0.95
4	300	10	0.35	0.60	1.71	1	1.25	1.25
5	300	10	0.40	0.60	1.50	1	1.69	1.69
6	300	10	0.45	0.60	1.33	1	2.42	2.42
7	300	10	0.50	0.60	1.20	1	3.86	3.86

Table 2. Initial data and results of calculation 2

№	T_0	P_0	P_1	P_2	P_2/P_1	$\dot{Q}_0$	$\dot{Q}_1$	$\dot{Q}_1/\dot{Q}_0$
	К	MPa	MPa	MPa	/	kg/s	kg/s	/
1	500	10	0.20	0.60	3.00	1	0.96	0.96
2	500	10	0.25	0.60	2.40	1	1.23	1.23
3	500	10	0.30	0.60	2.00	1	1.59	1.59
4	500	10	0.35	0.60	1.71	1	2.08	2.08
5	500	10	0.40	0.60	1.50	1	2.82	2.82
6	500	10	0.45	0.60	1.33	1	4.03	4.03
7	500	10	0.50	0.60	1.20	1	6.43	6.43

Table 3. Initial data and results of calculation 3

№	T_0	P_0	P_1	P_2	P_2/P_1	$\dot{Q}_0$	$\dot{Q}_1$	$\dot{Q}_1/\dot{Q}_0$
	K	MPa	MPa	MPa	/	kg/s	kg/s	/
1	623	10	0.20	0.60	3.00	1	1.06	1.06
2	623	10	0.25	0.60	2.40	1	1.37	1.37
3	623	10	0.30	0.60	2.00	1	1.77	1.77
4	623	10	0.35	0.60	1.71	1	2.32	2.32
5	623	10	0.40	0.60	1.50	1	3.13	3.13
6	623	10	0.45	0.60	1.33	1	4.47	4.47
7	623	10	0.50	0.60	1.20	1	7.15	7.15

The efficiency factors in calculations 1 and 2 are for the turbine $\eta_0 = 0.5$and the compressor $\eta_1 = 0{,}7$. The ratio of mass flow rates $\dot{q} = \dot{Q}_1/\dot{Q}_0$ in calculation 1 varies from 0.57 to 3.86 (Table 1). Calculation 2 considers the variant with working gas heating before entering the turbine. The working gas (methane) temperature at the turbine inlet $T_0 = 500$ K. The ratio of mass flow rates $\dot{q} = \dot{Q}_1/\dot{Q}_0$ varies in the range from 0.96 to 6.43 (Table 2).

In calculation 3, the working gas is superheated water steam (e.g., from a steam generator) and the pumped gas is methane (such as gas from a gas well with low reservoir pressure). The working gas temperature at the turbine inlet is $T_0 = 623$ K, the pumped gas (methane) temperature at the compressor inlet $T_1 = 300$ K, the gas constant for superheated steam $R_0 = 463$J/(kg*K) and methane $R_1 = 523$J/(kg*K), the adiabatic exponent for superheated steam k_0 =1.3, and the pressure variation range is 0.2 MPa≤ P_1 ≤0.5 MPa,isobaric heat capacity of superheated water steam c_{p0}=4012 J/(kg*K) at 10 MPa,efficiency factors for the turbine η_0=0,5 and compressor η_1=0,7,the ratios of mass flow rates $\dot{q} = \dot{Q}_1/\dot{Q}_0$ vary from 1.06 to 7.15 (Table 3). Here, the degree of pressure increases in the compressor 1,2 $\leq \pi_1 \leq$ 3 , where $\pi_1 = P_2/P_1$. Figure 11 shows the calculation dependences of $\dot{q}$ on π_1.

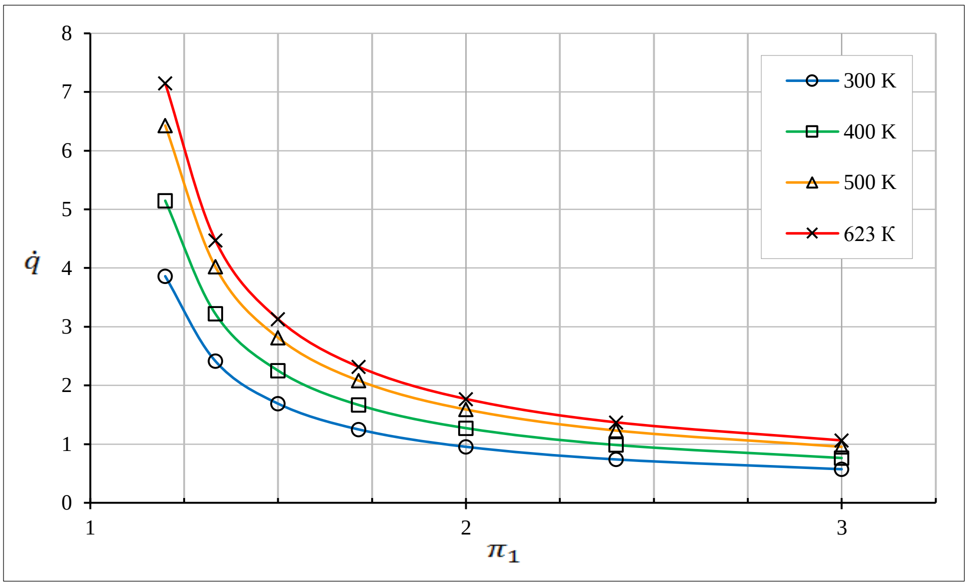

Figure 11. Calculation dependences of q˙ on π_1at different values of the working gas temperature: 300 K (calculation 1); 400 K; 500 K (calculation 2); 623 K (calculation 3)

At the late stage of developing gas fields, it is necessary to solve the relevant problem associated with booster compressor stations at the inlet pressure of P_1≤0.5 MPa. Under these conditions, it is difficult to provide cost-effective operation of expensive compressors at rapid change (decrease) of formation pressure at producing wells. However, at wells with high-reservoir pressure, gas energy loses and dissipates in the choke at the mouth of each such well. Eco-friendly gas energy from wells with high reservoir pressure can be used to operate a booster compressor station and for the cost-effective operating production wells with low-reservoir pressure. Calculations have shown (Figure 11) that it is possible to use methane and water steam as working gas separately or together for the turbomachine operation. By monitoring parameters of water steam, it is possible to adjust turbomachine operation mode to conditions of change in parameters of gas flows P_1 and P_0. It is well-known that turbines can also use propane or butane gas phase. These variants will make it possible to expand the regulation range of turbomachines and individual compressors.

Calculation 4 considers one example applied to a small aircraft (e.g., a UAV) on the possibility of increasing thrust and reducing fuel consumption by using atmospheric air in addition to the working gas from the gas generator. This example can use the scheme shown in Figures 9 and 10 and simultaneously implement two workflows – compressor and turbine in the turbomachine impeller. It would be logical to assume that such universality would entail some reduction in the energy efficiency of one or both of these workflows (compared with the optimized classical compressors and turbines). To quantify such considerations, it was decided to conduct a computational experiment to determine, in the first approximation, the level of turbine efficiency when a positive effect on the increase in thrust and decrease in fuel consumption can be expected to occur. The turbine efficiency η_0 served as a variable in these calculations.

The working hot gas from the gas generator comes to the turbine inlet at the pressure in the combustion chamber $P_0 = 0.9$ MPa. The working gas temperature at the turbine inlet $T_0 = 2000$ K, turbine outlet pressure $P_2 = 0.19$ MPa, and degree of pressure reduction $\pi_0 = 4.74$. The atmospheric air is the pumped gas. The air temperature at the compressor inlet is $T_1 = 300$ K, the compressor inlet pressure $P_1 = 0.1$ MPa and outlet pressure $P_2 = 0.19$ MPa, the degree of pressure increase $\pi_1 = 1.9$, and the compressor efficiency $\eta_1 = 0.7$. In this example, a mixture of working gas with atmospheric air from the zone with pressure $P_2 = 0.19$ MPa discharges into the atmosphere with pressure $P_1 = 0.1$ MPa. The symbol for the temperature of such a gas mixture at the outlet to the atmosphere is T_3.

Table 4 and Figure 12 show the individual calculation results.

Table 4. The results of calculation 4

η_0	T_3, K	$\dot{q}$	K_F	K_G
0.00	1663.72	0.00	0.60	1.67
0.05	1249.19	0.42	0.74	1.36
0.10	1022.26	0.83	0.86	1.16
0.20	781.01	1.66	1.09	0.91
0.30	654.58	2.50	1.31	0.76
0.40	576.76	3.33	1.53	0.65
0.50	524.03	4.16	1.74	0.58
0.60	485.94	4.99	1.94	0.52
0.70	457.15	5.82	2.14	0.47

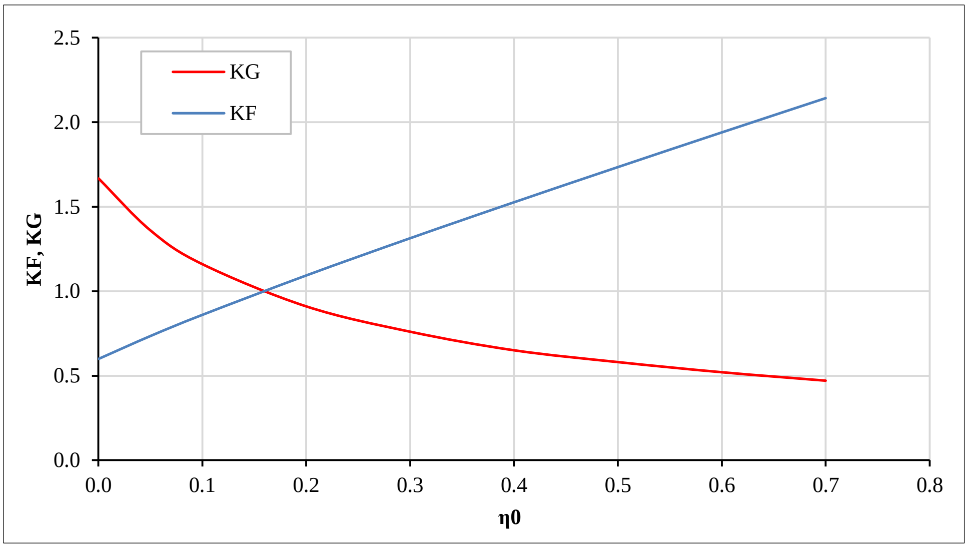

Figure 12. Calculation dependences of operating parameters in calculation 4

To analyze the calculation results, it is possible to introduce an additional parameter – coefficient of the fuel consumption change$K_G = G/G_0$, where G_0 – specific fuel consumption of gas generator [kg/(h×H)]; G – specific fuel consumption for the entire system, including the gas generator and connected turbomachine [kg/(h×H)].

The considered gas-dynamic system is open to using well-known technology for implementing afterburner modes to increase thrust. Figure 13 graphically shows the calculation results, considering the additional heat input from the chemical reaction of a hydrocarbon fuel with the oxygen of atmospheric air passing through the flow path of the hybrid turbomachine (in this calculation example, the heating value of hydrocarbon fuel was 30 MJ/kg). In this example, calculations show that the afterburner mode can increase the thrust twice compared with the mode without afterburner or can increase the thrust 4-fold compared with the option of a traditional gas generator provided that turbine efficiency is technically achievable at the level of $\eta_0 = 0.65$ in the combination with the compressor ($\eta_1 = 0.7$). Other examples and variants of hybrid turbomachines can be considered while continuing applied scientific research and solving optimization problems with the appropriate specification of working parameters.

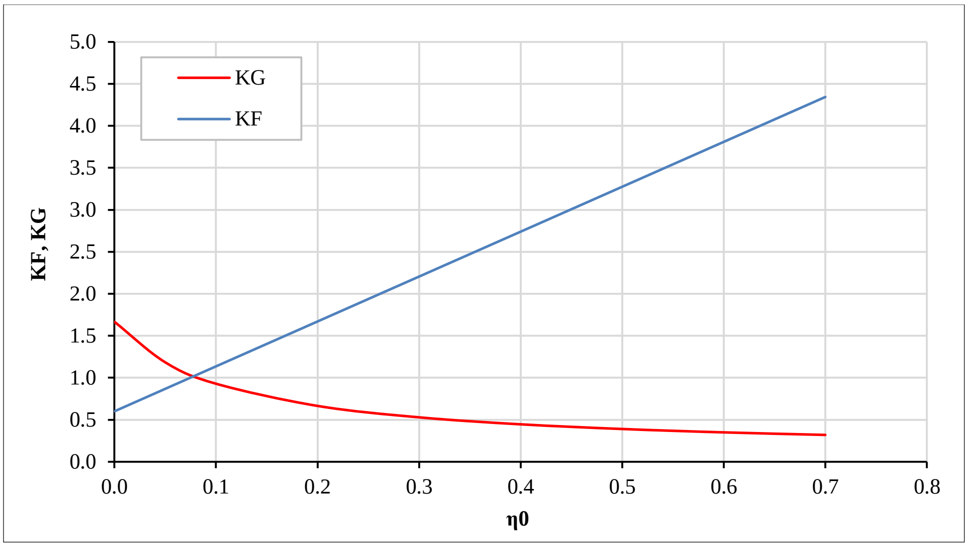

Figure 13. Calculation dependences of operating parameters (for afterburner operating mode)

The stage of patenting new technical solutions [6] included computer simulation (CFD) of a hybrid turbomachine. For example, Figures 14 and 15 graphically show selected CFD results.

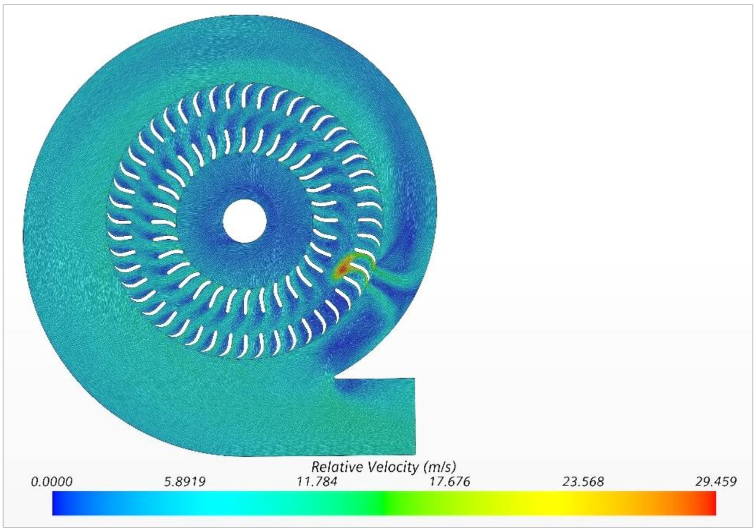

Figure 14. Results of computer simulation (example with liquid media)

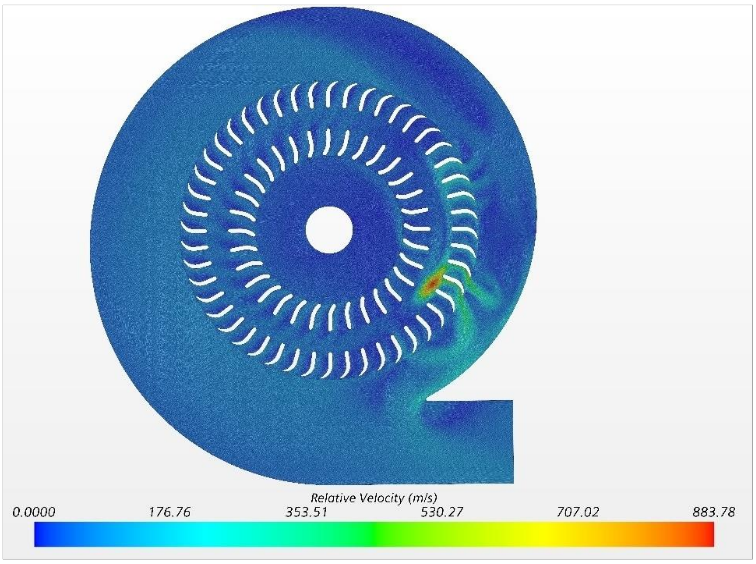

Figure 15. Results of computer simulation (example with gas media)

Numerical experiments were performed using the Star CCM+ software package. In the calculations, the model described by the averaged Reynolds Navier-Stokes equations with turbulence taken into account was used. The "k-e" turbulence model for any "y+" was applied. The total number of cells was about 1.5 million. We used a computer with the following parameters: CPU type: Intel(R) Core (TM) i7-10750U CPU @ 2.60GHz; RAM: 16 GB; Operating system: Windows 10. In this example, calculations (Figure 14) used a one-component incompressible medium (water). The working fluid flows to the turbine inlet at pressure $P_0 = 1{,}0$ MPa. The working and pumped liquid temperature at the turbine's inlet is $T_0 = 20°$C. The pressure at the turbine outlet is $P_2 = 0{,}1$ MPa. A variant of turbomachine operation in $P_1 = 0{,}1$ MPa mode has been considered. The ratio of mass flow rates $\dot{q} = \dot{Q}_1/\dot{Q}_0$, according to the calculation, was 4.828 at the impeller speed of 1750 rpm.

In the calculations (Figure 15), an ideal gas (air) model described by Reynolds averaged Navier-Stokes equations with turbulence taken into account was used. For a compressible medium with supersonic flows, "Coupled Flow" was used. Working gas at pressure $P_0 = 0{,}5$ MPa and temperature $T_0 = 2000$℃ is fed to the turbine inlet. The pressure at the outlet of the turbine is $P_0 = 0{,}5$ MPa. The variant of turbomachine operation in the turbofan mode at $P_2 = 0{,}1$ MPa is considered. The temperature of the pumped gas at the turbine inlet is $T_1 = 20°$C. The ratio of mass flows $\dot{q} = \dot{Q}_1/\dot{Q}_0$, according to calculation, was 7.235 at the impeller speed of 25,000 rpm.

The calculation results confirm the operability of the proposed and patented technical solution and show the prospect of developing applied scientific research in the field of hybrid turbomachines.

3.4. Some Generalizations

A summary of the results of scientific research performed in 2021 and 2022 [1–6] makes it possible to say the following:

- As part of developing Euler's ideas, a new scientific direction for the study of mesh turbomachines equipped with mesh jet control systems has been formed;
- For the first time, the issue of turbomachines, where the individual rotor blades alternately cyclically perform either the turbine function or the compressor (or pump) function, became subject to extensive discussion;
- For the first time, the issue of extreme conditions of a new mesh jet control system became subject to extensive discussion, and for the first time, it has been shown that at the nozzle outlet, the jet can deflect an angle from +180^o to –180^o within the geometric sphere.

The scope of the obtained results includes power engineering, oil and gas production, and processing. Some of the results apply to aviation and marine transportation systems. The obtained results also outlined the ways of developing new mesh engines where the fuel-air mixture combusts at constant volume or pressure using liquid, gaseous, or solid fuel.

The presented research paper solved the following main project tasks:

- It revealed promising directions for developing technologies and techniques using mesh turbomachines, which are possible to attribute to hybrid machines;
- It revealed new opportunities for improving the methodology of designing turbomachines within the training of modern designers because of the proposed novel modifications of turbomachines and a new direction of work for developing Euler's ideas.

It is well known that the class of turbomachines includes two subclasses: 1) "executing machines" and 2) "engine machines." Within the philosophy of engineering, other subclasses may exist. For educational purposes in training designers, the following additional subclasses of hybrid turbomachines are possible: "engine-executing machines," "driving machines," "gas-generator machines," "heat-exchanging machines," "mixing machines," and "separating machines." It is possible to consider the main workflow or several main workflows in a hybrid turbomachine (we are talking about several workflows occurring in one turbomachine impeller). In a hybrid turbomachine, it is possible to consider one or more energy sources, including sources operating on different physical principles.

4. Conclusions

4.1. Scientific Novelty

As part of developing Euler's ideas, a new scientific direction for studying and developing hybrid mesh turbomachines equipped with mesh jet control systems has been formed. It is well-known that the classification of turbomachines should reflect the level of historical development of this technique. But it is possible to suggest (wish): the classification of turbomachines should also reflect plans (possible variants) of turbomachine development, for example, hybrid turbomachines, so that a student or graduate student could see more clearly prospects to apply his forces in science and technology, and so a young scientist could also see the outlines of that "new," which is possible to create (but this "new" does not exist yet physically).

4.2. The Theoretical Contribution

The working hypothesis is put forward: "In the general case, in a turbomachine impeller, a separate blade can periodically participate in several workflows of energy transformation (or energy redistribution), in one fluid flow (the working body), or several flows of different fluids." This research has revealed the promising directions of theory development to create turbomachines, including hybrid ones, and new opportunities for the improvement of the methodology of turbomachine design to train designers.

4.3. Practical Significance

In current conditions, the most relevant problem is reducing energy costs to implement production processes, and in this regard, the role of turbomachines significantly increases. The scope of the obtained results includes power engineering, oil and gas production, and processing. Separate results apply to aviation and marine transport systems.

4.4. Limitations and Further Research

Limitations related to the difficulty of calculating nonstationary processes within the existing gas and fluid dynamics as applied to hybrid mesh turbomachines. At this research stage, the role of bench tests will be decisive in obtaining new scientific information. The research development can relate to evaluating the scientific and practical potential of hybrid mesh turbomachinery.

5. Declarations

5.1. Author Contributions

Conceptualization, Y.A.S.; methodology, M.A.M.; software, I.V.G.; validation, K.A.T.; formal analysis, V.V.V.; investigation, K.A.T.; resources, Y.A.S.; data curation, V.V.V.; writing—original draft preparation, N.N.B.; writing—review and editing, M.A.F.; visualization, I.V.G.; supervision, M.A.M.; project administration, M.A.M.; funding acquisition, Y.A.S. All authors have read and agreed to the published version of the manuscript.

5.2. Data Availability Statement

Data sharing is not applicable to this article.

5.3. Funding

The research was financially supported by the Russian Ministry of Education and Science within the framework of the government task in scientific activity, subject number FSZE-2020-0006.

5.4. Conflicts of Interest

The authors declare no conflict of interest.

6. References

[1] Sazonov, Y. A., Mokhov, M. A., Gryaznova, I. V., Voronova, V. V., Tumanyan, K. A., Frankov, M. A., & Balaka, N. N. (2021). Development and prototyping of jet systems for advanced turbomachinery with mesh rotor. Emerging Science Journal, 5(5), 775–801. doi:10.28991/esj-2021-01311.

[2] Sazonov, Y. A., Mokhov, M. A., Gryaznova, I. V., Voronova, V. V., Mulenko, V. V., Tumanyan, K. A., Frankov, M. A., & Balaka, N. N. (2021). Prototyping and study of mesh turbomachinery based on the Euler turbine. Energies, 14(17), 5292. doi:10.3390/en14175292.

[3] Sazonov, Y. A., Mokhov, M. A., Gryaznova, I. V., Voronova, V. V., Mulenko, V. V., Tumanyan, K. A., Frankov, M. A., & Balaka, N. N. (2021). Prototyping and study of jet systems for developing mesh turbomachines. International Review of Mechanical Engineering, 15(7), 335–345. doi:10.15866/ireme.v15i7.21163.

[4] Zeng, C., Xiao, Y., Luo, Y., Zhang, J., Wang, Z., Fan, H., & Ahn, S. H. (2018). Hydraulic performance prediction of a prototype four-nozzle Pelton turbine by entire flow path simulation. Renewable Energy, 125, 270-282. doi:10.1016/j.renene.2018.02.075.

[5] Sazonov, Y. A., Mokhov, M. A., Tumanyan, K. A., Frankov, M. A., & Balaka, N. N. (2020). Prototyping mesh turbine with the jet control system. Periódico Tchê Química, 17, 1160-117.

[6] Sazonov, Y. A., Mokhov, M. A., Tumanyan, K.A., Voronova, V. V., & Balaka, N. N. (2022). The utility model patent of the RF No. 213280 Useful model patent of the Russian Federation No 213280. Moscow, Russia. (In Russian).

[7] Yan, J., Zhang, C., Huo, S., Chai, X., Liu, Z., & Yan, K. (2021). Experimental and numerical simulation of bird-strike performance of lattice-material-infilled curved plate. Chinese Journal of Aeronautics, 34(8), 245–257. doi:10.1016/j.cja.2020.09.026.

[8] Di Caprio, F., Acanfora, V., Franchitti, S., Sellitto, A., & Riccio, A. (2019). Hybrid Metal/Composite Lattice Structures: Design for Additive Manufacturing. Aerospace, 6(6), 71. doi:10.3390/aerospace6060071.

[9] Boccini, E., Furferi, R., Governi, L., Meli, E., Ridolfi, A., Rindi, A., & Volpe, Y. (2019). Toward the integration of lattice structure-based topology optimization and additive manufacturing for the design of turbomachinery components. Advances in Mechanical Engineering, 11(8). doi:10.1177/1687814019859789.

[10] Zhang, Y., Li, F., & Jia, D. (2020). Lightweight design and static analysis of lattice compressor impeller. Scientific Reports, 10(1). doi:10.1038/s41598-020-75330-z.

[11] Magerramova, L., Volkov, M., Afonin, A., Svinareva, M., & Kalinin, D. (2018). Application of light lattice structures for gas turbine engine fan blades. Proccedings of the 31st Congress of the International Council of the Aeronautical Sciences, 9-14 September, 2018, Belo Horizonte, Brazil.

[12] Sajan, K. C., & Gautam, D. (2021). Progress in sustainable structural engineering: a review. Innovative Infrastructure Solutions, 6(2), 1-23. doi:10.1007/s41062-020-00419-3.

[13] Schülein, E., & Guyot, D. (2007). Wave Drag Reduction Approach for Lattice Wings at High Speeds. In New Results in Numerical and Experimental Fluid Mechanics VI, 332-339. Springer, Berlin, Germany. doi:10.1007/978-3-540-74460-3_41.

[14] Surawski, N. C., Macdonald, L. M., Baldock, J. A., Sullivan, A. L., Roxburgh, S. H., & Polglase, P. J. (2020). Exploring how fire spread mode shapes the composition of pyrogenic carbon from burning forest litter fuels in a combustion wind tunnel. Science of the total environment, 698, 134306.

[15] Ma, T., Wang, X., Qiao, N., Zhang, Z., Fu, J., & Bao, M. (2022). A Conceptual Design and Optimization Approach for Distributed Electric Propulsion eVTOL Aircraft Based on Ducted-Fan Wing Unit. Aerospace, 9(11), 690. doi:10.3390/aerospace9110690.

[16] Kazemi, E., & Luo, M. (2022). A comparative study on the accuracy and conservation properties of the SPH method for fluid flow interaction with porous media. Advances in Water Resources, 165, 104220. doi:10.1016/j.advwatres.2022.104220.

[17] Xue, Y., Wang, L., & Fu, S. (2018). Detached-eddy simulation of supersonic flow past a spike-tipped blunt nose. Chinese Journal of Aeronautics, 31(9), 1815–1821. doi:10.1016/j.cja.2018.06.016.

[18] Anbu Serene Raj, C., Narasimhavaradhan, M., Vaishnavi, N., Arunvinthan, S., Al Arjani, A., & Nadaraja Pillai, S. (2020). Aerodynamics of ducted re-entry vehicles. Chinese Journal of Aeronautics, 33(7), 1837–1849. doi:10.1016/j.cja.2020.02.019.

[19] Kini, C. R., Purohit, S., Bhagat, K. K., & Shenoy B., S. (2019). Effect of helix angle and cross section of helicoidal ducts in gas turbine blade cooling. International Review of Mechanical Engineering, 13(2), 87–96. doi:10.15866/ireme.v13i2.14942.

[20] Kini, C. R., Purohit, S., Bhagat, K. K., & Satish Shenoy, B. (2018). Heat transfer augmentation and cooling of a turbine blade using an innovative converging-diverging ducts - A CFD study. International Review of Mechanical Engineering, 12(7), 570–579. doi:10.15866/ireme.v12i7.15125.

[21] Yeranee, K., & RAO, Y. (2021). A review of recent studies on rotating internal cooling for gas turbine blades. Chinese Journal of Aeronautics, 34(7), 85–113. doi:10.1016/j.cja.2020.12.035.

[22] Deng, Q., Wang, H., He, W., & Feng, Z. (2022). Cooling Characteristic of a Wall Jet for Suppressing Crossflow Effect under Conjugate Heat Transfer Condition. Aerospace, 9(1). doi:10.3390/aerospace9010029.

[23] Kopiev, V. F., Belyaev, I. V., Dunayevsky, A. I., Pukhov, A. A., & Trofimovskiy, I. L. (2022). The Patent of the Russian Federation No. 2776193. Supersonic Aircraft, Bulletin 20, Moscow, Russia. (In Russian).

[24] Ji, Z., Zhang, H., & Wang, B. (2021). Thermodynamic performance analysis of the rotating detonative airbreathing combined cycle engine. Aerospace Science and Technology, 113, 106694. doi:10.1016/j.ast.2021.106694.

[25] Donateo, T., Spada Chiodo, L., Ficarella, A., & Lunaro, A. (2022). Improving the Dynamic Behavior of a Hybrid Electric Rotorcraft for Urban Air Mobility. Energies, 15(20), 7598. doi:10.3390/en15207598.

[26] Liu, B., Gao, Y., Gao, L., Zhang, J., Zhu, Y., Zang, X., & Zhao, J. (2022). Design and Experimental Study of a Turbojet VTOL Aircraft with One-Dimensional Thrust Vectoring Nozzles. Aerospace, 9(11), 678. doi:10.3390/aerospace9110678.

[27] Xia, J., & Zhou, Z. (2022). Model Predictive Control Based on ILQR for Tilt-Propulsion UAV. Aerospace, 9(11), 688. doi:10.3390/aerospace9110688.

[28] Wang, R., Zhang, G., Ying, P., & Ma, X. (2022). Effects of Key Parameters on Airfoil Aerodynamics Using Co-Flow Jet Active Flow Control. Aerospace, 9(11), 649. doi:10.3390/aerospace9110649.

[29] Decaix, J., & Münch-Alligné, C. (2022). Geometry, Mesh and Numerical Scheme Influencing the Simulation of a Pelton Jet with the OpenFOAM Toolbox. Energies, 15(19), 7451. doi:10.3390/en15197451.

[30] Asgarnejad, S., Kouhikamali, R., & Hassani, M. (2022). Triple-Nozzle Thermo-Compressor: Geometrical Investigation and Comparison with Single-Nozzle Thermo-Compressor. Journal of Applied Fluid Mechanics, 15(6), 1693–1702. doi:10.47176/jafm.15.06.1316.

[31] Seitz, A., Nickl, M., Troeltsch, F., & Ebner, K. (2022). Initial Assessment of a Fuel Cell—Gas Turbine Hybrid Propulsion Concept. Aerospace, 9(2). doi:10.3390/aerospace9020068.

[32] Zhou, S., Ma, H., Ma, Y., Zhou, C., & Hu, N. (2021). Experimental investigation on detonation wave propagation mode in the start-up process of rotating detonation turbine engine. Aerospace Science and Technology, 111, 106559 10 1016 2021 106559. doi:10.1016/j.ast.2021.106559.

[33] Sazonov, Y. A. (2012). Fundamentals of calculation and design of pump-ejector installations. SUE “Oil and Gas Publishing House” of Gubkin University: Moscow, Russia.

[34] Sazonov, Y., Mokhov, M., Tumanyan, K., Frankov, M., Voronova, V., & Balaka, N. Patent for utility model of the Russian Federation No. 214113. Jet Installation. Application, 2022116651, Moscow, Russia. (In Russian).

[35] Farassat, F., & Brentner, K. S. (1998). The acoustic analogy and the prediction of the noise of rotating blades. Theoretical and computational fluid dynamics, 10(1), 155-170. doi:10.1007/s001620050056.

[36] Sultanian, B. K. (2019). Logan's Turbomachinery: Flowpath Design and Performance Fundamentals. CRC Press, Florida, United States. doi:10.1201/9780203911600.